STRN-ALK rearranged pediatric malignant peritoneal mesothelioma – Functional testing of 527 cancer drugs in patient-derived cancer cells

Astrid Murumägi [a],[*], Daniela Ungureanu [b], Mariliina Arjama [a], Ralf Bützow [c], Jouko Lohi [c], Hannu Sariola [c], Jukka Kanerva [d], Minna Koskenvuo [d], Olli Kallioniemi [a],[e]

[a] Institute for Molecular Medicine Finland (FIMM), Helsinki Institute of Life Science (HiLIFE), University of Helsinki, Tukholmankatu 8, 00290 Helsinki, Finland
[b] Applied Tumor Genomics, Research Programs Unit, Faculty of Medicine and Health Sciences, University of Helsinki, Finland and Tampere University, Tampere, Finland
[c] Department of Pathology, University of Helsinki and Helsinki University Central Hospital, Helsinki, Finland
[d] Division of Hematology-Oncology and Stem Cell Transplantation, Children's Hospital and Helsinki University Central Hospital, Helsinki, Finland
[e] Science for Life Laboratory (SciLifeLab), Department of Oncology and Pathology, Karolinska Institute, Solna, Sweden

ARTICLE INFO

ABSTRACT

Genetic rearrangements involving the anaplastic lymphoma kinase (ALK) gene create oncogenic drivers for several cancers, including malignant peritoneal mesothelioma (MPeM). Here, we report genomic and functional precision oncology profiling on a rare case of a 5-year old patient diagnosed with wide-spread and aggressive MPeM, driven by STRN-ALK rearrangement. We established genomically representative patient-derived cancer cells (PDCs) from the tumor sample and performed high-throughput drug sensitivity testing with 527 oncology compounds to identify potent inhibitors. As expected, the PDCs were overall sensitive to the ALK inhibitors, although the eight different inhibitors tested had variable efficacy. We also discovered other effective inhibitors, such as MEK/ERK inhibitors and those targeting pathways downstream of ALK as well as Bcl-xl inhibitors. In contrast, most cytotoxic drugs were not very effective. ALK inhibitors synergized with MEK and PI3K/mTOR inhibitors, highlighting potential combinatorial strategies to enhance drug efficacy and tackle drug resistance. Based on genomic data and associated functional validation, the patient was treated with the ALK inhibitor crizotinib in combination with conventional chemotherapy (cisplatin and gemcitabine). A complete disease remission was reached, lasting now for over 3 years. Our results illustrate a rare pediatric cancer case, and highlight the potential of functional precision oncology to discover pathogenetic drivers, validate dependency on driver signals, compare different inhibitors against each other and potentially enhance targeted treatments by drug combinations. Such real-time implementation of functional precision oncology could pave the way towards safer and more effective personalized cancer therapies for individual pediatric cancer patients with rare tumors.

1. Introduction

Chromosomal rearrangements involving anaplastic lymphoma kinase (ALK) are known oncogenic drivers encompassing multiple cancers, including lymphomas and non-small-cell lung cancer [1]. These translocations involve diverse fusion partners that enable ALK autophosphorylation resulting in constitutively active tyrosine kinase that leads to aberrant activation of its downstream signaling pathways, such as RAS/ERK, PI3K/AKT and JAK/STAT [2]. Five ALK tyrosine kinase inhibitors have been approved by the Food and Drug Administration (FDA) and European Medicines Agency (EMA) thus far. These include the first-

generation ALK inhibitor crizotinib (Xalkori), second-generation ALK inhibitors alectinib (Alecensa), brigatinib (Alunbrig) and ceritinib (Zykadia), and recently approved third-generation ALK inhibitor lorlatinib (Lorviqua) [3]. In addition, several other ALK-targeting compounds are currently in preclinical or clinical development phases [4]. The administration of ALK inhibitors has produced remarkable clinical responses, however, often these have not been durable, due to the development of resistance [5].

Fusion partner striatin (STRN) gene resulting in STRN-ALK was first reported in 2014 in thyroid cancer and since then has been also detected in non-small-cell lung cancer, colorectal cancer, malignant mesothe-

lioma and recently in salivary intraductal carcinoma [6–10]. *STRN-ALK* is a rare fusion gene, which mechanistically leads to constitutive activation of ALK tyrosine kinase and aberrant activation of several downstream signaling pathways such as MAPK/PI3K/STAT3 driving tumor progression [2,7].

Here, we report detection of *STRN-ALK* fusion in a 5-year old pediatric patient diagnosed with widely spread malignant peritoneal mesothelioma (MPeM). Although occurrence of MPeM in young patients is rare, *STRN-ALK* fusion has been reported before such as in a 12-year old MPeM patient [11]. Hung et al. analyzed the prevalence of ALK fusions in adult MPeM and identified that 3% of patients in their cohort were ALK-positive, suggesting that ALK rearrangements play a role in MPeM pathogenesis [8]. MPeM is a rare and aggressive cancer, affecting the mesothelial tissue of the peritoneum, pericardium and tunica vaginalis, with rare metastatic spread beyond the abdominal cavity [12]. The disease is associated with poor prognosis due to late diagnosis and the median survival is less than 12 months for the majority of patients. The standard first-line treatment is cytoreductive surgery (CRS) with heated intraperitoneal chemotherapy (HIPEC). There are also novel agents in clinical trials such as inhibitors of the epidermal growth factor receptor, vascular endothelial growth factor, mesothelin, and histone deacetylases [12,13].

The application of functional *ex vivo* testing of patient-derived cancer cells (PDCs) with a panel of oncology drugs has been suggested and applied for predicting the patients´ clinical response to targeted therapeutics. This is complementary to the standard precision oncology approach, which relies on the identification of actionable mutations of driver oncogenes by next-generation sequencing [14,15]. Here, we applied our functional precision medicine approach by integrating molecular profiling data of cancer cells with the phenotypic drug response profile of PDCs *ex vivo* to explore therapeutic options for this rare cancer form. These data were then passed to the clinicians and could be considered in helping the patient treatment regimens. Our results revealed selective efficacy of several ALK inhibitors towards patients´ PDCs *ex vivo* in 2D as well as in 3D condition. In addition, we identified several synergistic drug combinations that had stronger effect on cell viability than ALK inhibitors alone. Combinations could be useful to prevent drug resistance from arising and hence, therapeutic efficacy and durability of the response.

2. Material and methods

2.1. Establishment of patient-derived cancer cell culture

The patient material and clinical data were acquired under Institutional Ethical Review Board-approved protocol (Dnro HUS/1880/2017) and in accordance with the Declaration of Helsinki. Informed consent was obtained from the patient´s parent, including a permission to publish the patient case. Primary patient-derived cancer cell (PDC) culture designated as FM-MPeM-01 was established from diagnostic tumor biopsies. Briefly, fresh biopsies were processed to obtain single-cell suspension by enzymatic digestion using a Tumor Dissociation kit (Miltenyi Biotec) and gentleMACS Dissociator (Miltenyi Biotec). PDCs were established and maintained in RPMI-1640 media (Gibco) supplemented with hEGF (20 ng/ml), hydrocortisone (1 μg/ml), primocin (Invivogen) and 5 % FBS at 37°C with 5% CO$_2$. Majority of non-cancerous cells, mainly stromal cells (referred to as Mixed culture) were removed during the establishment of PDCs by differential trypsinization and maintained in RPMI-1640 media supplemented with 5% FBS and primocin (Invivogen) at 37°C with 5% CO$_2$. All experiments were performed with low (<10) passage cells and the culture was routinely tested for mycoplasma contamination using mycoplasma detection kit QuickTest (Biotool) according the manufacturer´s instructions.

2.2. Immunohistochemistry (IHC) and fluorescence in situ hybridization (FISH)

Tumor biopsy samples were formalin fixed and paraffin embedded in the HUSLAB Pathology department according to standard procedures. For IHC analysis, formalin-fixed paraffin-embedded (FFPE) blocks were cut as 3.5μm sections and stained for antibodies against ALK (#3633, Cell Signaling Technology), CK7 (clone OV-TL 12/30, Agilent Dako), calretinin (clone DAK-Calret 1, Agilent Dako), WT1 (#83535, Cell Signaling Technology), CK5/6 (clone D5/16 B4, Agilent Dako), PAX8 (#10336-1-AP, ProteinTech,) and ER (clone 1D5, Agilent Dako) using protocols for routine diagnostics. IHC stained sections were scanned with a high-resolution whole-slide scanner (Pannoramic 250 Flash III, 3DHISTECH) with a x20 objective. The ALK rearrangement status of the tumor biopsy sample was evaluated by FISH in the HUSLAB Genetics laboratory using ALK dual-color break-apart probe according to manufacturer's protocol (Vysis, Abbott Molecular)

2.3. RT-PCR and sanger sequencing

Total RNA was isolated from FM-MPeM-01 PDCs using RNeasy kit (Qiagen) and the quality of the RNA was assessed with Qubit fluorometer (Thermo Fisher Scientific). 3 micrograms of total RNA was used for the first strand cDNA synthesis using the High Capacity cDNA Reverse Transcription Kit (Applied Biosystems). RT-PCR was performed with Phusion Flash High-Fidelity PCR master mix (Thermo Fisher Scientific). Verification of *STRN-ALK* fusion gene in FM-MPeM-01 PDCs was carried out at the FIMM Technology Centre Sequencing Unit by capillary sequencing. Primer sequences were the following: forward primer 5´- CCACAAGTTGAAATACGGGACA and reverse primer 5´- ACTGATG-GAGGAGGTCTTGC.

2.4. Immunofluorescence

Cells were cultured on 384-well high content imaging plates (PerkinElmer) and fixed with 4% PFA in PBS solution for 15 min at RT. Permeabilization was done with 0.1% Triton X in PBS for 10 min at RT followed by 1 h blocking with 1% BSA in PBS. After washing with PBS, cells were incubated overnight at 4°C with CK7 (Clone OV-TL 12/30, Dako), pan-cytokeratin (ab9377, Abcam) and PDGF Receptor-β (#3169, Cell Signaling Technologies) antibodies followed by secondary antibodies, Alexa Fluor 488 Goat Anti-Mouse IgG (#A-11001) and Alexa Fluor Plus 594 donkey anti-rabbit IgG (#A32754, Invitrogen, Thermo Fisher Scientific), incubation for 1h at RT. The cells were counterstained with Hoechst 33342 (Invitrogen, Thermo Fisher Scientific). Images were taken with PerkinElmer Opera Phenix automatic spinning-disk confocal microscope using a 20 x water objective, NA 1.0.

2.5. Western blot

Whole cell lysates were prepared from FM-MPeM-01 PDCs and Mixed culture grown in 2D by lysing cells in ice cold lysis buffer (50 mM Tris-HCl pH 7.5, 10 % glycerol, 150mM NaCl, 1 mM EDTA, 1% Triton-x-100, 50 mM NaF) supplemented with protease and phosphatase inhibitor cocktails (Biotool). Cell lysates were incubated 20 min on ice followed by 20 min centrifugation at 4°C. Cell pellets were resuspended in SDS sample buffer and proteins were separated by sodium dodecyl sulfate polyacrylamide gel electrophoresis (SDS–PAGE) and transferred to nitrocellulose membranes. After blocking (5% BSA in 0.05% Tween20 in 1xTBS) at RT for 1h, blots were incubated with the indicated primary antibodies overnight at 4°C. Blots were washed three times with 1xTBS/0.1%Tween20 buffer and incubated with secondary antibodies for 1h at RT. Blots were scanned with Odyssey CLx Imaging System (LI-COR) and images were processed with Image Studio Lite (LI-COR). Following antibodies were used for western blot: ALK (#3633), phospho-ALK (Tyr1282/1283, #3714), phospho-MEK1/2 (Ser217/221,

#9121), ERK1/2 (#4696), phospho-ERK1/2 (Thr202/Tyr204, #9101), phospho-JNK (Thr183/Tyr185, #9255), JNK (#9252) from Cell Signaling Technology; MEK1/2 (#sc-6250) and β-tubulin (#sc-166729) from Santa Cruz Biotechnology. As secondary antibodies IRDye 800CW Donkey anti-Mouse IgG or IRDye 680RD Donkey anti-Rabbit IgG (LI-COR) at 1:10000 dilution were used.

2.6. Drug sensitivity and resistance testing (DSRT)

DSRT was performed with FM-MPeM-01 PDCs and Mixed culture with FIMM FO5 drug library containing 527 approved and investigational drugs (Supplemental Table S1A) as described previously [15]. Briefly, the drugs were dissolved in 100% dimethyl sulfoxide or water and plated in five concentrations covering a 10,000-fold range on 384-well flat clear bottom tissue culture treated microplates (Corning) using an Echo 550 acoustic dispenser (Labcyte). Cells were dispensed on pre-drugged plates with the Multidrop dispenser (Thermo Fisher Scientific) and incubated for 72 hours at 37°C at 5% CO_2. Cell viability was measured with Cell Titer-Glo Cell Viability Assay (Promega). Quantitative dose response curves for each drug were generated as previously described [15]. The drug efficacy was quantified with a modified area-under-the-curve measurement called drug sensitivity score (DSS), calculated and visualized as previously described [16,17]. For measuring the drug responses for ALK inhibitors in 3D culture conditions, the assay was carried out similarly, except PDCs or Mixed culture were seeded on ultra-low attachment 384-well round bottom cell culture plates (Corning) pre-plated with drugs in nine increasing concentrations. Drug combination testing was performed with selected drugs using drug concentration matrices covering seven different concentrations. Highest single agent (HSA) synergy model was applied for synergy assessment using the R package SynergyFinder [18].

3. Results

3.1. The patient's clinicopathological features

A 5-year old patient was referred to the Helsinki University Central Hospital because of weight loss, mild anemia and a rise in C-reactive protein levels (CRP). Abdominal ultrasound and magnetic resonance imaging (MRI) showed a large pelvic tumor mass and a second tumor mass in the upper abdomen infiltrating to the liver (Fig. 1A). The tumor mass had also spread below the spleen across the omentum and was surrounded by ascites. The whole-body MRI, lung computed tomography (CT) and positron emission tomography-computed tomography (PET-CT) scans did not show any extra-abdominal metastasis. For diagnostic purposes tumor biopsies were taken, however, primary operation was not possible because of the diffuse spread in abdomen. Conventional chemotherapy with cisplatin and gemcitabine was started. The immunohistochemistry (IHC) analysis of multiple tumor biopsies revealed that cancer cells stained positive for cytokeratin-7 (CK7) as well as Wilms' tumor protein 1 (WT1), calretinin and cytokeratin 5/6 (CK5/6), which are markers frequently detected in both mesotheliomas and serous carcinomas (Supplemental Fig. S1) [19]. Furthermore, tumor cells were also positive for the expression of paired box-protein (PAX8) and estrogen receptor (ER), which are usually markers for serous ovarian cancer (Supplemental Fig. S1). Taken together, the morphology based on hematoxylin and eosin staining and the immunohistopathologic analysis of the tumor biopsies prompted us to establish a diagnosis of MPeM (Fig. 1B). Next-generation sequencing of the tumor biopsy with a targeted Foundation One cancer panel revealed a *STRN-ALK* fusion gene and in line with this finding, we detected a strong ALK expression by IHC (Fig. 1C) and a chromosomal fusion event by fluorescence in situ hybridization (FISH) (Fig. 1D) in tumor sample. *STRN-ALK* translocation is formed by exon 3 of *STRN* and exon 20 of *ALK*, retaining the ALK tyrosine kinase domain in the fusion protein, as reported also for other patient cases with the same fusion [6,7,11]. Besides the identification

of *STRN-ALK* fusion, the tumor was microsatellite stable and showed no other driver mutations and had a low overall mutation burden.

3.2. Drug sensitivity testing on representative patient-derived cancer cells

Fresh tumor biopsy obtained for diagnostic purposes was processed to establish a patient-derived cancer cell (PDC) culture designated as FM-MPeM-01 for functional analyses (Supplemental Fig. S2A). In parallel, primary cell culture consisting of mainly fibroblasts with few cancer cells referred as a Mixed culture was also established from the same biopsy sample (Supplemental Fig. S2B). FM-MPeM-01 PDCs stained positive for CK7 and pan-cytokeratin, which exhibited weak staining for these markers in Mixed culture (Supplemental Fig. S3). In contrast, Mixed culture cells were positive for PDGF β-receptor, commonly expressed in fibroblasts (Supplemental Fig. S3) [20]. To confirm the molecular identity of PDCs with the original tumor sample, FM-MPeM-01 PDCs were analyzed for the expression of *STRN-ALK* fusion gene by RT-PCR and Sanger sequencing, ALK expression by IHC and expression of representative proteins of signaling pathways activated by ALK hyperactivation such as phospho-MEK, phospho-ERK, phospho-JNK, by Western blotting (Fig. 1E and F, Supplemental Fig. 2C and D). Western blot analysis showed the absence of phospho-ALK and lower expression of its downstream phospho-MEK/phospho-ERK in the Mixed culture cell lysates compared to the PDCs (Supplemental Fig. S2D). To determine the drug response profile of FM-MPeM-01, the PDCs and Mixed culture cells were studied by a high-throughput drug sensitivity and resistance testing (DSRT) platform with a panel of 527 approved drugs and emerging oncology compounds (Fig. 2A, Supplemental Table S1B). In addition to the Mixed culture, as another control, we used DSRT data from two healthy bone marrow samples. To identify FM-MPeM-01 PDC-selective drug efficacies, we correlated the drug responses of the PDC in relation to both Mixed culture and healthy bone marrow samples (Fig. 2B). We considered a selective drug sensitivity score (sDSS) above 5 as a hit. DSRT data revealed that FM-MPeM-01 PDCs were sensitive to ALK inhibitors, as expected. From eight ALK inhibitors included in the drug library, six displayed selective cancer cell-specific sensitivity, including all approved ALK inhibitors, with brigatinib, ensartinib and crizotinib exhibiting highest sensitivities (Fig. 2C, Supplemental Fig. S4). Alectinib had a lower sDSS compared to the Mixed culture (sDSS 4.5), but had a higher sDSS compared to bone marrow control samples (sDSS 5.4). The corresponding values for CEP-37440 were 4 and 7.9, respectively. Among other drugs displaying selective sensitivity in FM-MPeM-01 PDC were apoptotic inhibitors (such as navitoclax and investigational compounds A-1155463 and A-1331852) and small molecule kinase inhibitors targeting MAPK signaling pathway components (pan-RAF inhibitors TAK-530, cobimetinib and trametinib) (Fig. 2B-D, Supplemental Fig. S4). In contrast, most cytotoxic drugs were not very effective, including gemcitabine and cisplatin (Supplemental Fig. S5).

We also evaluated drug responses of PDCs grown in both 2D and 3D conditions. We defined sensitivity to the eight ALK inhibitors in the FM-MPeM-01 PDC cultured as 3D spheroids (Supplemental Fig. 2A, Supplemental Table S1C and S1D). FM-MPeM-01 PDCs displayed a higher sensitivity to ALK inhibitors in 3D as compared to 2D, confirming the dependency of the cancer cells to ALK hyperactivation driven oncogenic signaling (Fig. 3). Six ALK inhibitors had DSS between 15 to 20.8, with brigatinib displaying highest sensitivity (DSS 20.8), followed by ceritinib and crizotinib. A second-generation approved ALK inhibitor, alectinib, had lower response to FM-MPeM-01 PDCs, as compared to other drugs, resulting in only 50% cell viability reduction in 3D assay as well as lower response in 2D (Fig. 3).

3.3. Identification of effective drug combinations targeting FM-MPeM-01 PDCs

Inhibiting cancer-associated pathways with a single agent has often proven to have limited clinical efficacy due to the development of resis-
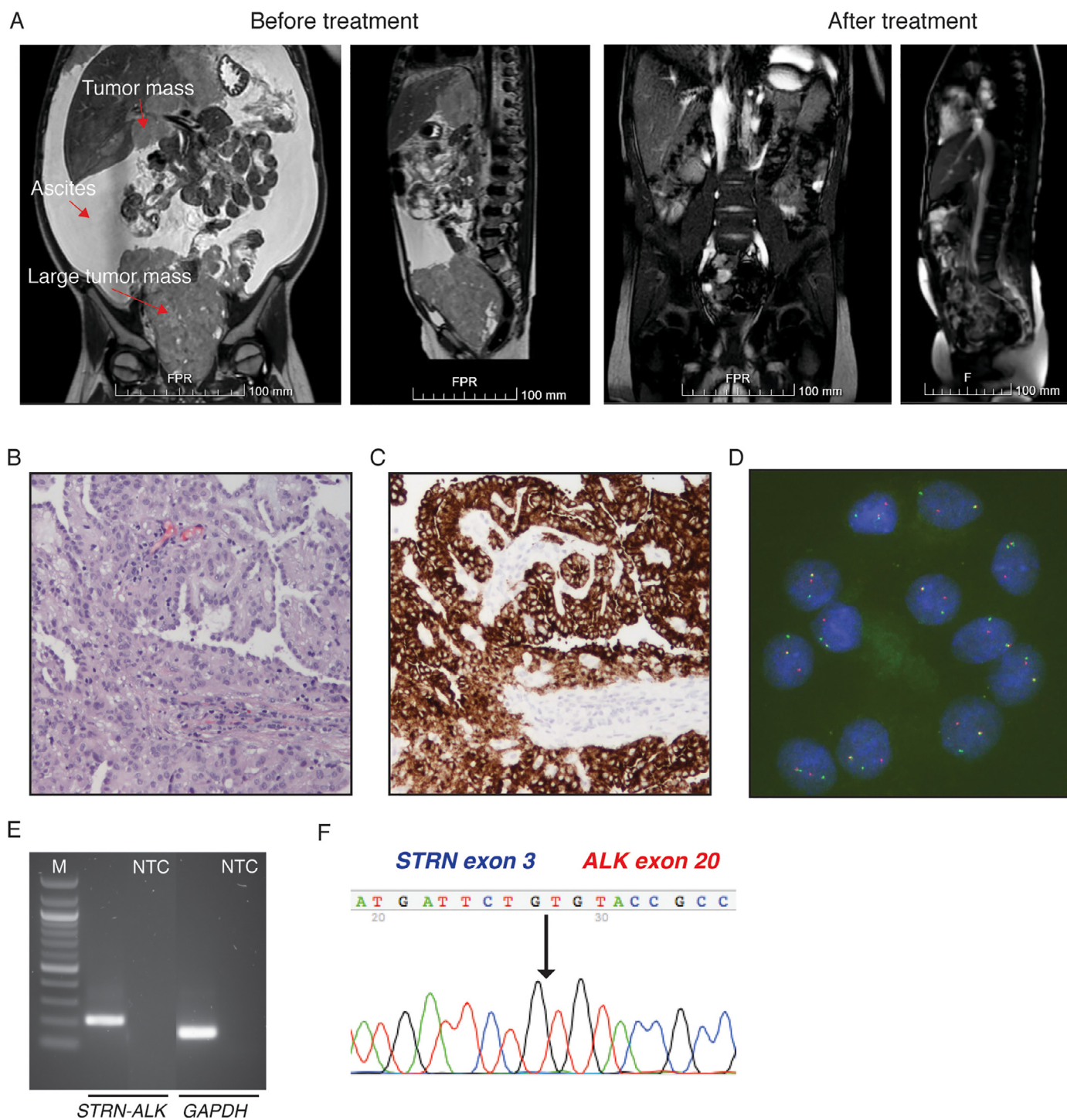
Fig. 1. Clinical profile and molecular characterization of the tumor. (A) Gadolinium-enhanced magnetic resonance image (MRI) scans of the patient´s abdomen before and after one year of treatment with chemotherapy and crizotinib. Images before the treatment showed a large pelvic mass and a mass infiltrating the liver surrounded by ascites (as indicated by red arrows). Follow-up images after one year of treatment with crizotinib in combination with chemotherapy, including tumor resection after 4 months of crizotinib combination treatment, shows complete disease remission. (B) Representative hematoxylin and eosin stained section of the tumor biopsy (original magnification x 10) (C) Representative IHC staining shows strong ALK expression in the tumor tissue (original magnification x 10). (D) Representative FISH image (100 x) showing ALK rearrangement (split red and green signals) in the tumor cells nuclei. (E) Confirmation of the *STRN-ALK* transcript in patient-derived cancer cells by RT-PCR. Also shown are size marker (M) and no-template control (NTC); and Sanger sequencing (F). Partial chromatogram showing the *STRN-ALK* transcript nucleic acid sequence where the break-point is indicated by an arrow.
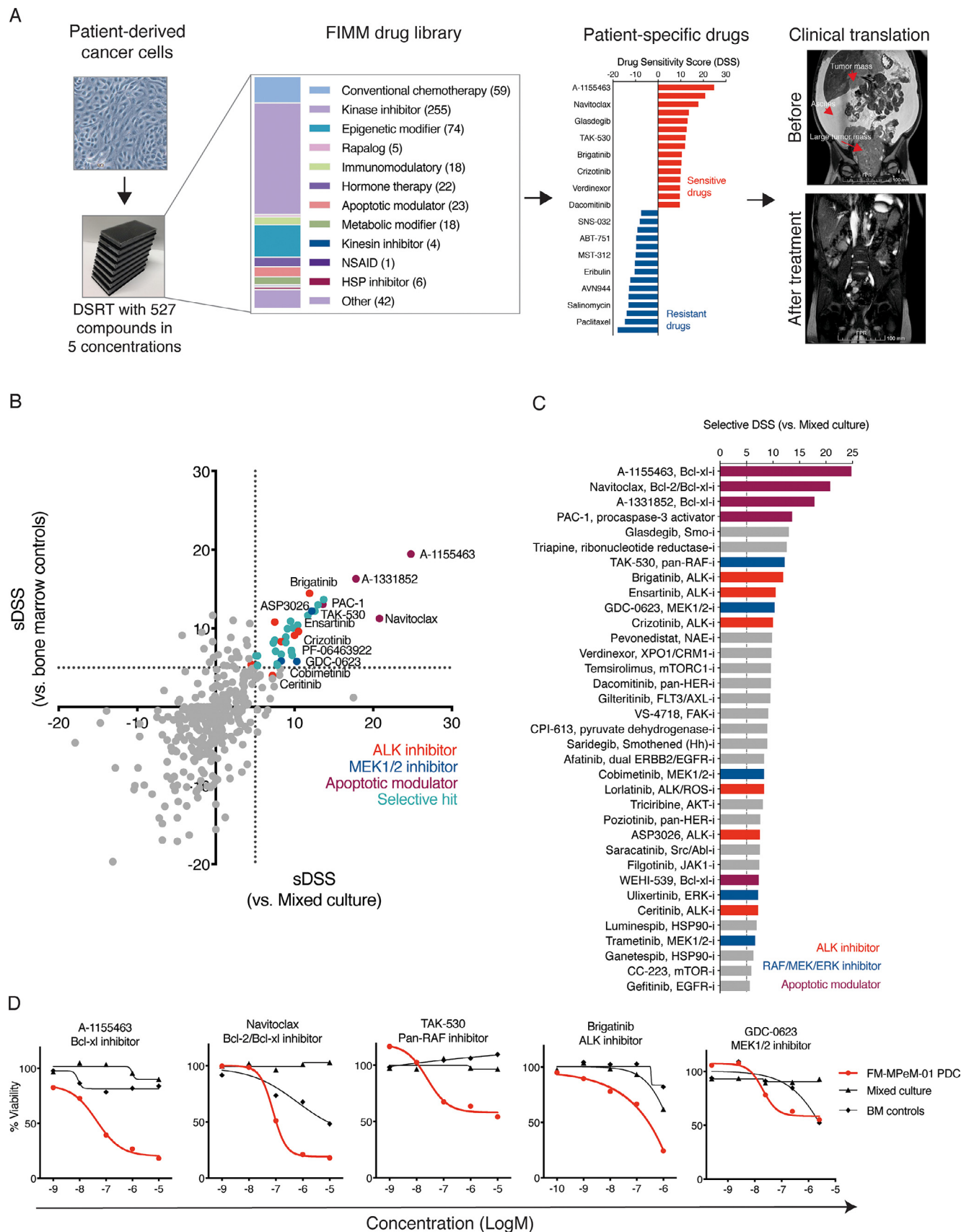
Fig. 2. Drug sensitivity profile of FM-MPeM-01 PDCs. (A) Schematic representation of the functional drug sensitivity testing platform where patient-derived cancer cells (PDCs) established from tumor biopsy are tested in the drug sensitivity and resistance (DSRT) assay with 527 drugs to identify patient-specific drug sensitivities. (B) Scatter plot showing the selective drug sensitivity (sDSS) scores of FM-MPeM-01 PDC in relation to healthy bone marrow controls (Y-axis) and Mixed culture (X-axis). ALK inhibitors are highlighted in red, MEK1/2 inhibitors in blue, apoptotic modulators in purple and other selective hits in turquoise. (C) Bar-plot graph showing the sDSS towards Mixed culture of the most effective drugs for FM-MPeM-01 PDCs. Highlighted are ALK inhibitors (red), RAF/MEK/ERK inhibitors (blue) and apoptotic modulators (purple). FM-MPeM-01 PDCs and Mixed culture cells underwent drug testing with 527 drugs at five concentrations for 72 hours. Cell viability was measured with the CellTiter-Glo luminescent cell viability assay. (D) Individual dose-response curves for drugs displaying higher selective responses in FM-MPeM-01 PDCs compared to Mixed culture and healthy bone marrow (BM) controls.
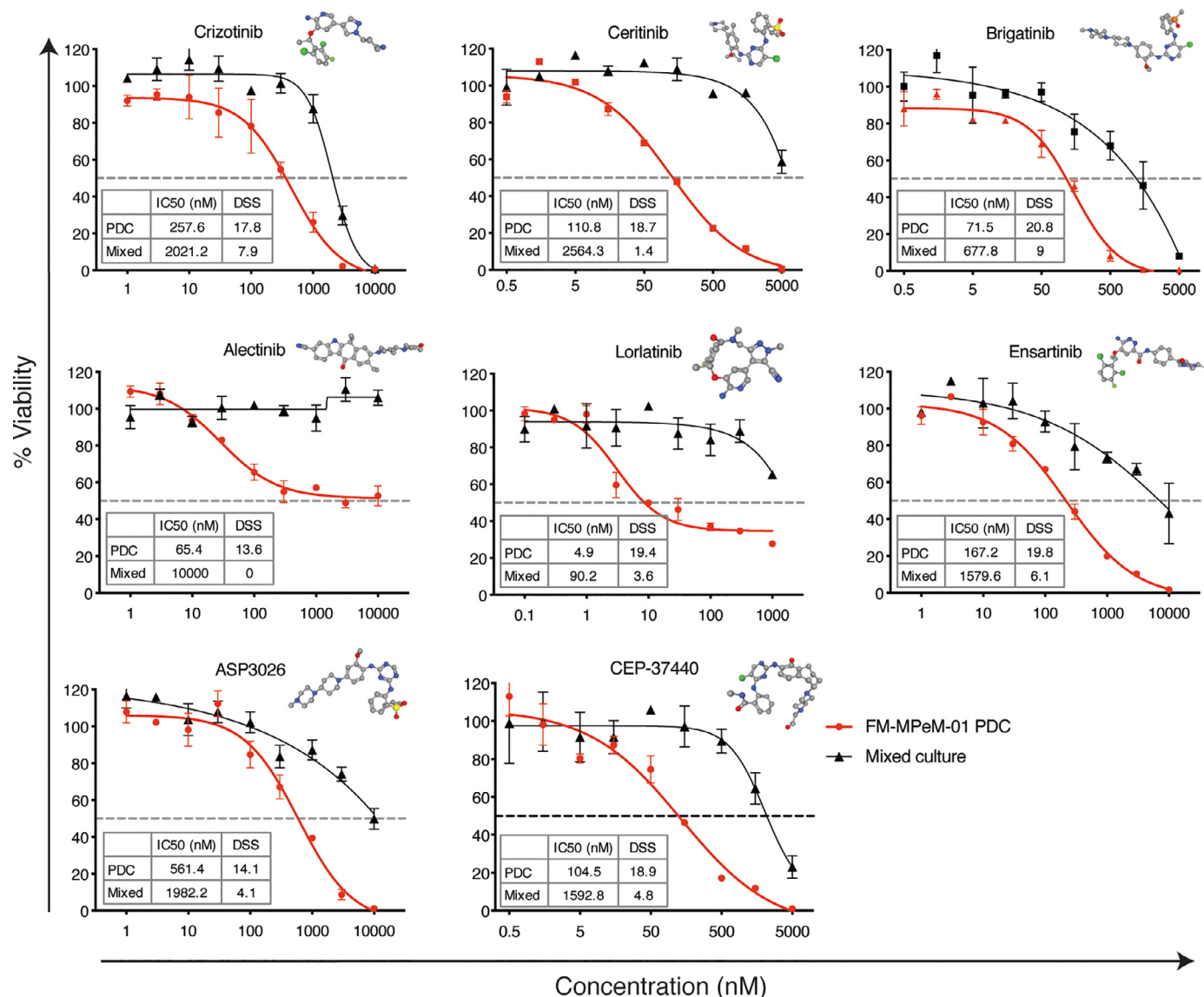
Fig. 3. Different efficacies of ALK inhibitors towards FM-MPeM-01 PDCs in 3D. Dose-response curves for eight ALK inhibitors for FM-MPeM-01 PDCs and Mixed culture tested in 3D condition as spheroids. Individual IC50 and DSS values are shown for each drug, which were tested in 9 concentrations. Average of two replicates is shown with the error bars. 3D structure is shown for each drug based on PubChem.

tance, as it has been shown also for ALK-driven cancers [1]. Combining drugs inhibiting several oncogenic signaling pathways is considered a more effective way to kill cancer cells and achieve remission [21]. Consequently, we tested various drug combinations targeting MAPK, PI3K and STAT pathways that are known to be upregulated in ALK-rearranged cancers [2]. Drug combinations were tested on a dose-response matrix in seven concentrations and the SynergyFinder, a web-based application to analyze drug combination data, was used to detect any potential synergy [22]. We identified strong synergy between ALK inhibitors (crizotinib and ceritinib) in combination with MEK (cobimetinib) and mTOR/PI3K (gedatolisib) inhibitors, respectively (Fig. 4). The synergy was more efficient for ceritinib compared to crizotinib. These results highlight the potential efficacy of these combinations in ALK-positive MPeM cancer treatment if the resistance to ALK-targeting monotherapy would rise; in addition, the value of *ex vivo* PDCs in testing novel therapeutic agents and their combinations preclinically.

3.4. Patient response to personalized treatments

Taking into consideration both molecular profiling and the validation by *ex vivo* drug sensitivity testing, crizotinib 1200 mg/week i.e. 11

mg/kg/day was added to the neoadjuvant chemotherapy combination treatment (cisplatin 60 mg/m^2 and gemcitabine 2000 mg/m^2 per cycle). The patient received six cycles of this combination. Six months after initial diagnosis and treatment with a combination of chemotherapy and crizotinib, the residual tumor was resected. At the time of the resection, the pathological examination of the residual tumor revealed a small percentage of intact tumor cells. The treatment was continued after the surgery for two cycles, followed by crizotinib monotherapy lasting for one year, until complete remission was achieved. In total, the patient received crizotinib 1200 mg/week i.e. approximately 11 mg/kg/day for about 20 months. Currently, three-years after the initial diagnosis and 16 months after completion of treatment, there are no signs of residual tumor by MRI and the patient is otherwise a healthy 8-year old girl presenting normal growth and development.

4. Discussion

Here we present the application of a genomic and functional precision medicine approach to identify and validate targeted treatment for a 5-year old pediatric patient case with a rare advanced MPeM carrying
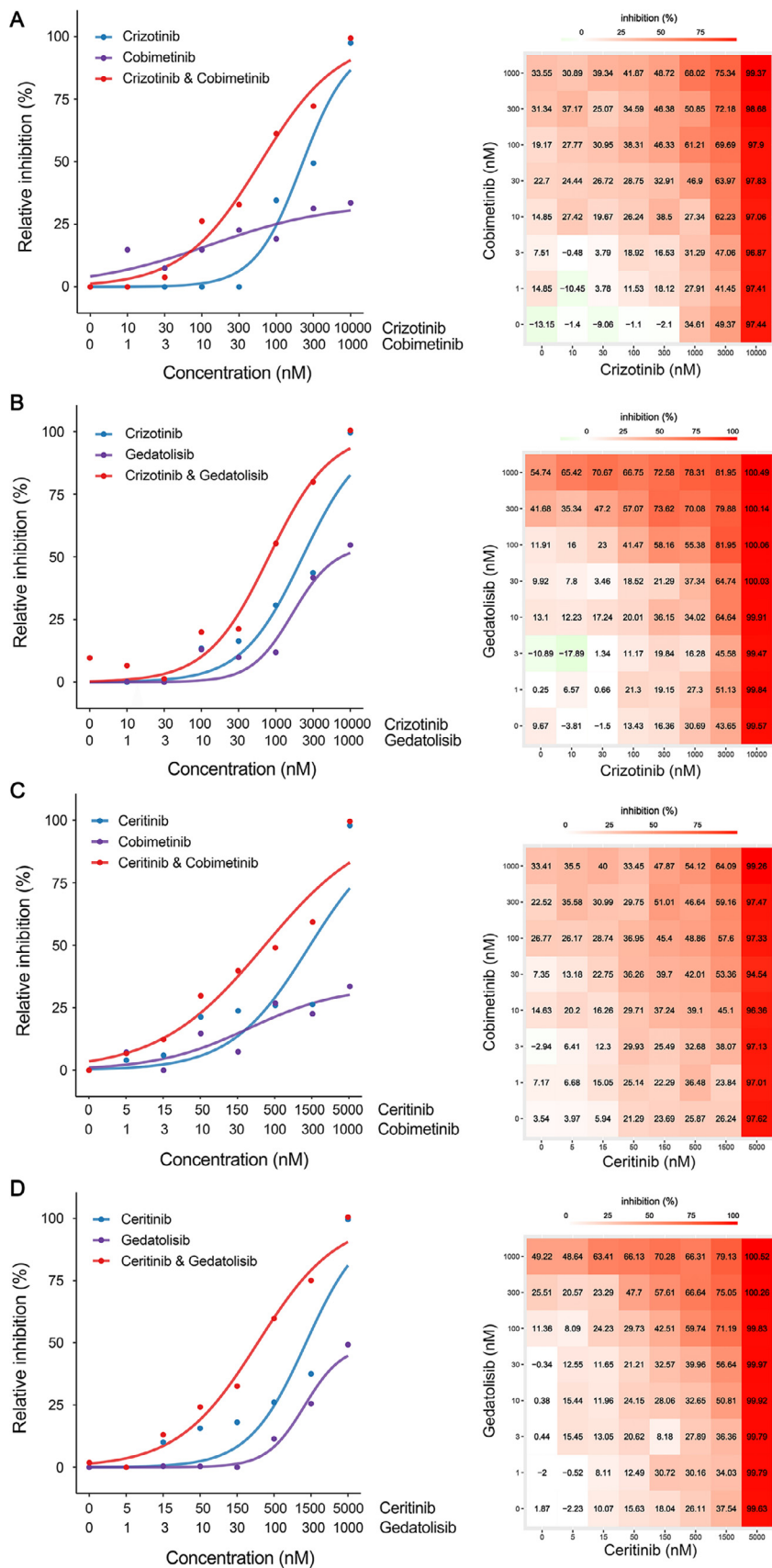
Fig. 4. Targeting MEK and ALK or MEK and PI3K/mTOR synergistically inhibits FM-MPeM-01 PDCs growth. Dose-response curves of ALK inhibitors crizotinib (A, B) and ceritinib (C, D) alone or in combination with MEK inhibitor cobimetinib (A and C) and PI3K/mTOR inhibitor gedatolisib (B and D) in FM-MPeM-01 PDCs measured with cell viability assay after three days. Shown is one representative experiment of at least two replicates.

STRN-ALK fusion gene. Crizotinib treatment, along with chemotherapy led to complete disease remission, now lasting for over 3 years.

Detection of *ALK*-rearrangements in MPeM suggests that for a small subgroup of patients with this cancer, encompassing particularly pediatric cases, these fusions act as a driver of tumorigenesis making the tumor sensitive to targeted therapy [8,11,23]. *STRN-ALK* fusion was recently reported in another 12-year old MPeM pediatric patient case who had excellent response to second-generation ALK inhibitor ceritinib [11]. Promising ALK inhibitor responses have been reported also in other tumor types with *STRN-ALK* fusion [7,24–26]. However, in one report with this fusion detected in NSCLC, the patient was resistant to ALK inhibitor alectinib [6]. To date, more than 30 different ALK 5′fusion partner genes have been identified and ALK translocations involving different partners and even different fusion points with the same partner demonstrate distinct sensitivity to the structurally different ALK inhibitors [27]. Childress et al. [27] studied seven distinct ALK-fusions (*STRN-ALK* was not included) and showed that the 5′ partner affected the biochemical and cellular properties of the ALK fusion protein, including kinase activity, protein stability, and, importantly, response to ALK inhibitor. Therefore, we consider it was relevant to test the efficacy of eight ALK inhibitors, including approved and investigation ones, towards FM-MPeM-01 PDCs. While all were efficacious, there was variability between the inhibitors. Crizotinib and ceritinib are both ATP-competitive ALK tyrosine kinase inhibitors, except that crizotinib is also a selective c-MET inhibitor and ceritinib inhibits also other receptors with lesser degree, such as IGF-1, insulin receptor and ROS [28,29]. Ceritinib was highly effective in patients with advanced, *ALK*-rearranged NSCLC, including those who had had disease progression during crizotinib treatment, indicating its efficacy as a second-generation ALK inhibitor [29]. Moreover, alectinib and brigatinib are also next-generation ALK inhibitors, showing superior activity over chemotherapy and crizotinib in recent studies in ALK-rearranged NSCLC [30,31].

Precision cancer therapy using *ex vivo* pharmacological testing of PDCs has shown great potential in identifying clinically translatable treatments, especially for hematological malignancies [15,32]. Therefore, functional testing of targeted drugs and drug combinations in PDCs could provide valuable confirmation of genomics-based precision medicine. PDCs established from solid tumor tissue or ascites may represent a relevant model for predicting drug efficacy of patients, and they can help to dissect molecular mechanisms of drug dependency across a panel of similar or different drugs as well as their combinations [33,34]. With our high-throughput drug testing platform we analyzed the response profile of FM-MPeM-01 PDCs to 527 drugs, including approved oncology drugs and investigational compounds. We showed that FM-MPeM-01 PDCs were sensitive to all eight ALK inhibitors included in the drug panel, both in 2D and 3D conditions. This finding supported the clinical use of ALK inhibitor in patient treatment. Three ALK inhibitors were approved by EMA in Europe at the time, crizotinib and newly approved alectinib and ceritinib. From these, crizotinib was chosen to be included for treatment based on clinical availability of the drug at the local pediatric hospital. The patient responded well to the targeted treatment and has now been in remission for three years from diagnosis, including a year after completion of treatment. Functional drug testing with PDCs revealed cancer cell vulnerabilities also to other targeted inhibitors beyond ALK, such as apoptotic inhibitors and MEK inhibitors. Since acquired resistance to ALK inhibitors is a major obstacle in treating ALK-positive cancers, combination therapies that could improve ALK inhibitors efficacy warrant further research. We investigated this synergy in our FM-MPeM-01 PDC model using MEK, PI3K and JAK inhibitors. Combination treatment of ALKi with either MEK (cobimetinib) or PI3K (gedatolisib) inhibitors had a higher inhibitory effect in our FM-MPeM-01 PDC model than ALK inhibitors alone, indicating that simultaneous targeting of ALK and MEK or PI3K signaling pathway could potentially improve the efficacy of ALK inhibitors in MPeM and also could be explored in a clinical trial for patient treatment.

5. Conclusions

In summary, we have demonstrated the feasibility of PDCs and the relevance of functional drug testing in highlighting opportunities for personalized cancer treatment.

Declaration of Competing Interest

O.K. is a co-founder and a board member of Medisapiens and Sartar Therapeutics and has received royalty on patents licensed by Vysis-Abbot. His research group has a Vinnova-funded collaborative program with Astra-Zeneca, Labcyte, Takara Biosciences and Pelago, which are not related to this work. Other authors did not disclose any potential conflicts of interest.

Supplementary materials

Supplementary material associated with this article can be found, in the online version, at doi:10.1016/j.tranon.2021.101027.

References

[1] Z Cao, Q Gao, M Fu, N Ni, Y Pei, WB. Ou, Anaplastic lymphoma kinase fusions: Roles in cancer and therapeutic perspectives, Oncol Lett 17 (2) (2019) 2020–2030, doi:10.3892/ol.2018.9856.

[2] SP Ducray, K Natarajan, GD Garland, SD Turner, G. Egger, The transcriptional roles of ALK fusion proteins in tumorigenesis, Cancers (Basel) 11 (8) (2019), doi:10.3390/cancers11081074.

[3] A Sgambato, F Casaluce, P Maione, C. Gridelli, Targeted therapies in non-small cell lung cancer: a focus on ALK/ROS1 tyrosine kinase inhibitors, Expert Rev Anticancer Ther 18 (1) (2018) 71–80, doi:10.1080/14737140.2018.1412260.

[4] DC Ziogas, A Tsiara, G Tsironis, M Lykka, M Liontos, A Bamias, Treating ALK-positive non-small cell lung cancer, Ann Transl Med 6 (8) (2018) 141, doi:10.21037/atm.2017.11.34.

[5] B Golding, A Luu, R Jones, AM. Viloria-Petit, The function and therapeutic targeting of anaplastic lymphoma kinase (ALK) in non-small cell lung cancer (NSCLC), Mol Cancer 17 (1) (2018) 52, doi:10.1186/s12943-018-0810-4.

[6] Y Nakanishi, S Masuda, Y Iida, N Takahashi, S. Hashimoto, Case report of non-small cell lung cancer with STRN-ALK translocation: a nonresponder to alectinib, J Thorac Oncol 12 (12) (2017) e202–e2e4, doi:10.1016/j.jtho.2017.08.009.

[7] LM Kelly, G Barila, P Liu, VN Evdokimova, S Trivedi, F Panebianco, Identification of the transforming STRN-ALK fusion as a potential therapeutic target in the aggressive forms of thyroid cancer, Proc Natl Acad Sci U S A 111 (11) (2014) 4233–4238, doi:10.1073/pnas.1321937111.

[8] YP Hung, F Dong, JC Watkins, V Nardi, R Bueno, P Dal Cin, Identification of ALK rearrangements in malignant peritoneal mesothelioma, JAMA Oncol 4 (2) (2018) 235–238, doi:10.1001/jamaoncol.2017.2918.

[9] LM Rooper, LDR Thompson, J Gagan, BR Oliai, I Weinreb, JA. Bishop, Salivary intraductal carcinoma arising within intraparotid lymph node: a report of 4 cases with identification of a novel STRN-ALK fusion, Head Neck Pathol (2020), doi:10.1007/s12105-020-01198-0.

[10] G Perot, I Soubeyran, A Ribeiro, B Bonhomme, F Savagner, N Boutet-Bouzamondo, Identification of a recurrent STRN/ALK fusion in thyroid carcinomas, PLoS One 9 (1) (2014) e87170, doi:10.1371/journal.pone.0087170.

[11] JH Rüschoff, E Gradhand, A Kahraman, H Rees, JL Ferguson, A Curioni-Fontecedro, STRN-ALK rearranged malignant peritoneal mesothelioma with dramatic response following ceritinib treatment, JCO Precision Oncology (3) (2019) 1–6, doi:10.1200/po.19.00048.

[12] J Kim, S Bhagwandin, DM. Labow, Malignant peritoneal mesothelioma: a review, Ann Transl Med 5 (11) (2017) 236, doi:10.21037/atm.2017.03.96.

[13] F Nicolini, M Bocchini, G Bronte, A Delmonte, M Guidoboni, L Crino, Malignant pleural mesothelioma: state-of-the-art on current therapies and promises for the future, Front Oncol 9 (2019) 1519, doi:10.3389/fonc.2019.01519.

[14] A. Letai, Functional precision cancer medicine-moving beyond pure genomics, Nat Med 23 (9) (2017) 1028–1035, doi:10.1038/nm.4389.

[15] T Pemovska, M Kontro, B Yadav, H Edgren, S Eldfors, A Szwajda, Individualized systems medicine strategy to tailor treatments for patients with chemorefractory acute myeloid leukemia, Cancer Discov 3 (12) (2013) 1416–1429, doi:10.1158/2159-8290.CD-13-0350.

[16] B Yadav, T Pemovska, A Szwajda, E Kulesskiy, M Kontro, R Karjalainen, Quantitative scoring of differential drug sensitivity for individually optimized anticancer therapies, Sci Rep 4 (2014) 5193, doi:10.1038/srep05193.

[17] S Potdar, A Ianevski, JP Mpindi, D Bychkov, C Fiere, P Ianevski, Breeze: an integrated quality control and data analysis application for high-throughput drug screening, Bioinformatics 36 (11) (2020) 3602–3604, doi:10.1093/bioinformatics/btaa138.

[18] A Ianevski, L He, T Aittokallio, J. Tang, SynergyFinder: a web application for analyzing drug combination dose-response matrix data, Bioinformatics 33 (15) (2017) 2413–2415, doi:10.1093/bioinformatics/btx162.

[19] F Lin, H. Liu, Immunohistochemistry in undifferentiated neoplasm/tumor of uncertain origin, Arch Pathol Lab Med 138 (12) (2014) 1583–1610, doi:10.5858/arpa.2014-0061-RA.

[20] J Paulsson, T Sjoblom, P Micke, F Ponten, G Landberg, CH Heldin, Prognostic significance of stromal platelet-derived growth factor beta-receptor expression in human breast cancer, Am J Pathol 175 (1) (2009) 334–341, doi:10.2353/ajpath.2009.081030.

[21] AS Crystal, AT Shaw, LV Sequist, L Friboulet, MJ Niederst, EL Lockerman, Patient-derived models of acquired resistance can identify effective drug combinations for cancer, Science 346 (6216) (2014) 1480–1486, doi:10.1126/science.1254721.

[22] A Ianevski, L He, T Aittokallio, J. Tang, SynergyFinder: a web application for analyzing drug combination dose-response matrix data, Bioinformatics 36 (8) (2020) 2645, doi:10.1093/bioinformatics/btaa102.

[23] K Loharamtaweethong, N Puripat, N Aoonjai, A Sutepvarnon, C. Bandidwattanawong, Anaplastic lymphoma kinase (ALK) translocation in paediatric malignant peritoneal mesothelioma: a case report of novel ALK-related tumour spectrum, Histopathology 68 (4) (2016) 603–607, doi:10.1111/his.12779.

[24] H Ren, X Hou, PW Eiken, J Zhang, KE Pierson, AA Nair, Identification and development of a lung adenocarcinoma PDX model with STRN-ALK fusion, Clin Lung Cancer 20 (2) (2019) e142–e1e7, doi:10.1016/j.cllc.2018.11.002.

[25] Y Yang, SK Qin, J Zhu, R Wang, YM Li, ZY Xie, A Rare STRN-ALK fusion in lung adenocarcinoma identified using next-generation sequencing-based circulating tumor DNA profiling exhibits excellent response to crizotinib, Mayo Clin Proc Innov Qual Outcomes 1 (1) (2017) 111–116, doi:10.1016/j.mayocpiqo.2017.04.003.

[26] H Kusano, Y Togashi, J Akiba, F Moriya, K Baba, N Matsuzaki, Two cases of renal cell carcinoma harboring a novel STRN-ALK fusion gene, Am J Surg Pathol 40 (6) (2016) 761–769, doi:10.1097/PAS.0000000000000610.

[27] MA Childress, SM Himmelberg, H Chen, W Deng, MA Davies, CM. Lovly, ALK fusion partners impact response to ALK inhibition: differential effects on sensitivity, cellular phenotypes, and biochemical properties, Mol Cancer Res 16 (11) (2018) 1724–1736, doi:10.1158/1541-7786.MCR-18-0171.

[28] NM Nix, KS. Brown, Ceritinib for ALK-rearrangement-positive non-small cell lung cancer, J Adv Pract Oncol 6 (2) (2015) 156–160.

[29] AT Shaw, JA. Engelman, Ceritinib in ALK-rearranged non-small-cell lung cancer, N Engl J Med 370 (26) (2014) 2537–2539, doi:10.1056/NEJMc1404894.

[30] T Hida, H Nokihara, M Kondo, YH Kim, K Azuma, T Seto, Alectinib versus crizotinib in patients with ALK-positive non-small-cell lung cancer (J-ALEX): an open-label, randomised phase 3 trial, Lancet 390 (10089) (2017) 29–39, doi:10.1016/S0140-6736(17)30565-2.

[31] DR Camidge, HR Kim, JC Yang, JY Han, JS Lee, Brigatinib versus crizotinib in ALK-positive non-small-cell lung cancer, N Engl J Med 379 (21) (2018) 2027–2039, doi:10.1056/NEJMoa1810171.

[32] MM Majumder, R Silvennoinen, P Anttila, D Tamborero, S Eldfors, B Yadav, Identification of precision treatment strategies for relapsed/refractory multiple myeloma by functional drug sensitivity testing, Oncotarget 8 (34) (2017) 56338–56350, doi:10.18632/oncotarget.17630.

[33] K Saeed, V Rahkama, S Eldfors, D Bychkov, JP Mpindi, B Yadav, Comprehensive drug testing of patient-derived conditionally reprogrammed cells from castration-resistant prostate cancer, Eur Urol 71 (3) (2017) 319–327, doi:10.1016/j.eururo.2016.04.019.

[34] DP Kodack, AF Farago, A Dastur, MA Held, L Dardaei, L Friboulet, Primary patient-derived cancer cells and their potential for personalized cancer patient care, Cell Rep 21 (11) (2017) 3298–3309, doi:10.1016/j.celrep.2017.11.051.